J. Plasma Phys. (2026), *vol*. 92, E40 © The Author(s), 2026. Published by Cambridge University Press. This is an Open Access article, distributed under the terms of the Creative Commons Attribution-NonCommercial-NoDerivatives licence (https://creativecommons.org/licenses/by-nc-nd/4.0/), which permits non-commercial re-use, distribution, and reproduction in any medium, provided that no alterations are made and the original article is properly cited. The written permission of Cambridge University Press or the rights holder(s) must be obtained prior to any commercial use and/or adaptation of the article.
doi:10.1017/S0022377826101354

Extended envelope nonlinear waves in dusty plasma chain

Lan-Xin Shi[1], Wei-Ping Zhang[1], Zhong-Zheng Li[2], Yang-Yang Yang[3], Juan-Fang Han[1] and Wen-Shan Duan[1]

[1]College of Physics and Electronic Engineering, Northwest Normal University, Lanzhou 730070, PR China
[2]School of Energy and Power Engineering, Gansu Minzu Normal University, Hezuo 747000, PR China
[3]Institute of Modern Physics, Chinese Academy of Sciences, 509 Nanchang Road, Lanzhou 730000, PR China

Corresponding author: Wen-Shan Duan, duanws@126.com

(Received 26 August 2025; revision received 17 October 2025; accepted 28 January 2026)

The present paper originates from the need to understand nonlinear wave behaviour in dusty plasmas, aiming to explore stable envelope wave propagation and interactions beyond traditional theoretical models. By using nonlinear Schrödinger equation (NLSE) analysis and molecular dynamics (MD) simulations, the study verifies the existence and stable propagation of non-standard envelope waves. It demonstrates elastic like collisions, introduces tuneable parameters for wave shaping and quantifies error trends with nonlinearity. A key breakthrough is confirming that even analytically invalid waveforms remain stable, challenging NLSE constraints. Present results enhance nonlinear wave theory and support precise, tuneable signal transmission in plasma diagnostics and microgravity experiments.

Key words: complex plasmas, strongly coupled plasmas

1. Introduction

Dusty plasma is a system composed of electrons, ions, neutral particles and charged dust grains (Du *et al.* 2012; Thomas *et al.* 2016; Davletov, Kurbanov & Mukhametkarimov 2020; Beckers *et al.* 2023; Lu *et al.* 2025; Williams *et al.* 2025). Current research on dusty plasmas primarily focuses on several areas, including dust-related phenomena in natural environments such as planetary rings (Havnes *et al.* 1995; Gong *et al.* 2021; Jiang & Du 2022) and the mesosphere (Sternovsky *et al.* 2004; Popel & Dubinsky 2013), various plasma–particle interactions (Shukla & Eliasson 2009; Kompaneets, Morfill & Ivlev 2016), particle growth and fusion in industrial applications (Santos *et al.* 2019; Nespoli *et al.* 2022), many-body physics (Thoma *et al.* 2023), and fundamental problems in condensed matter (Morfill & Ivlev 2009; Chaudhuri *et al.* 2011). Over the past decades, one of the most significant breakthroughs in dusty plasma physics has been the experimental

discovery of dust lattice structures (Hayashi & Tachibana 1994; Chu & Lin 1994; Melzer, Trottenberg & Piel 1994; Thomas *et al.* 1994). Subsequently, dust lattice waves were observed within these ordered systems (Melandsø 1996; Homann *et al.* 1997). This discovery not only confirmed that dust particles can spontaneously form crystal-like ordered structures under strongly coupled conditions, but also provided a solid foundation for the study of wave propagation and collective behaviours in dusty plasmas.

In 1996, Melandsø (1996) first investigated wave propagation in one-dimensional dusty plasma lattices, and this theoretical work laid the foundation for subsequent experimental studies. Then, Homann *et al.* (1997) experimentally observed dust lattice waves and subsequently extended the study to two-dimensional dusty plasma systems (Homann *et al.* 1998). Huang *et al.* (2019) first investigated the square lattice structures in two-dimensional binary complex plasmas, and then Singh *et al.* (2022) achieved the observation of a square lattice formation in a monodisperse complex plasma system. The propagation characteristics of linear waves have been extensively investigated through experiments, theoretical analyses and numerical simulations (Vladimirov, Shevchenko & Cramer 1997; Otani, Bhattacharjee & Wang 1999; Ivlev & Morfill 2000; Misawa *et al.* 2001; Nunomura *et al.* 2002; Liu, Avinash & Goree 2003; Farokhi, Kourakis & Shukla 2006; Wang *et al.* 2006; Bandyopadhyay *et al.* 2008; Farokhi & Hameditabar 2012; Lipaev *et al.* 2025). In recent years, research has gradually shifted towards nonlinear phenomena in dust lattice waves, including solitary waves (Avinash *et al.* 2003; Sheridan, Nosenko & Goree 2008; Tian-Jun 2009; Ghosh & Gupta 2010; Hong *et al.* 2021; Wei *et al.* 2023*a*; Huang *et al.* 2023), shock waves (Ghosh 2008*a*,*b*, 2009; Kananovich & Goree 2020; Niu, Tian & Chen 2020; Ding *et al.* 2021; Wei *et al.* 2023*b*) and breathers (Kourakis & Shukla 2005; Koukouloyannis & Kourakis 2009; Koukouloyannis *et al.* 2010). These nonlinear phenomena have attracted considerable attention due to their significance in energy transport applications and wave dynamics control in controlled environments.

In the field of nonlinear wave research, envelope waves, as a significant nonlinear structures, have garnered considerable attention in dusty plasma lattice systems (Ivlev, Zhdanov & Morfill 2003; Kourakis & Shukla 2004, 2006; Togueu Motcheyo *et al.* 2018; Nkendji Kenkeu *et al.* 2022; Houwe *et al.* 2022; Shi *et al.* 2024; Han *et al.* 2025). Togueu Motcheyo *et al.* (2018) numerically demonstrated that envelope bright solitons can propagate stably within dusty plasma lattices. Subsequently, Houwe *et al.* (2022) further investigated the propagation dynamics of envelope solitons under vertical oscillations of dust grains based on the nonlinear Schrödinger equation (NLSE). They elucidated the formation mechanisms of bright and dark solitons in different frequency regimes and confirmed the validity of their theoretical predictions through numerical simulations. Notably, envelope waves have been extensively studied not only in dusty plasma lattices, but also across various disciplines, including fluid mechanics (Osborne 2002; Slunyaev *et al.* 2013; Gandzha & Sedletsky 2017; Stepanyants 2019; Liao *et al.* 2023) and nonlinear optics (Karjanto 2022; Wazwaz *et al.* 2023; Omar *et al.* 2025). These interdisciplinary efforts have provided a solid theoretical foundation for understanding the formation and evolution of envelope waves. However, most existing studies on envelope solitons are restricted to analytical solutions of the NLSE. In this work, we overcome this limitation by employing numerical simulations. We demonstrate the existence of bright solitons that do not conform to the standard analytical envelope bright soliton solutions of the NLSE, and systematically investigate their propagation characteristics

https://doi.org/10.1017/S0022377826101354 Published online by Cambridge University Press

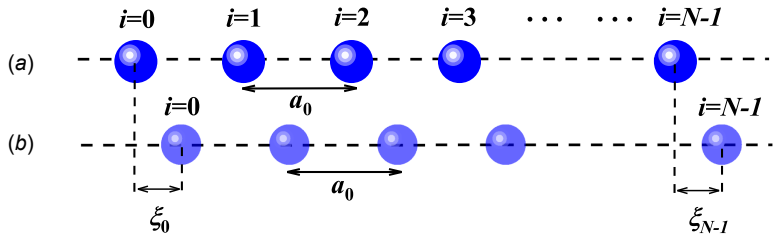


FIGURE 1. Schematics of a dust particle chain, in which the blue spheres are dust particles labelled from $i = 0$ to $i = N - 1$. (*a*) Arrangement of dust particles at their equilibrium positions, with a_0 denoting the lattice constant; (*b*) Configuration when the dust particles are displaced from their equilibrium position, where ξ_i represents the displacement of the ith dust particle from its equilibrium position.

and stability. This discovery significantly advances the theoretical framework of nonlinear waves in dusty plasmas and other nonlinear systems.

The rest of this paper is organised as follows. In § 2, establishes the model used for the present study. In § 3, a systematic investigation is conducted on the propagation properties and stability of arbitrarily prescribed envelope waves and general waveforms in a one-dimensional dusty plasma chain. Section 4 presents the conclusion for the present paper.

2. Model

We consider an homogeneous dust particle chain in which all particles are identical within the range $i = 0$ to $i = N - 1$, as illustrated in figure 1. The present study focuses on what kind of the envelope waves exists in the system.

The position of the ith dust particle is assumed to be $x_i = ia_0 + \xi_i$, where ξ_i represents the displacement from its equilibrium position ia_0 and a_0 is the lattice constant. The equation of motion governing an arbitrary dust particle i is given by $m_d\ddot{\xi}_i = -Q_d\nabla\sum_{j\neq i}\phi_{ij}$, where m_d and Q_d are the mass and charge of the dust particle, ϕ_{ij} is the Yukawa interaction potential between dust particles of i and j, $\phi_{ij} = (Q_d/4\pi\varepsilon_0 x_{ij})e^{-x_{ij}/\lambda_D}$, where $x_{ij} = |x_i - x_j|$ is the distance between dust particles i and j, λ_D is the Debye length, and ε_0 is the permittivity of vacuum.

By using the small amplitude approximation $a_0 \gg \xi_i - \xi_{i-1}$, the long-wavelength approximation $a_0 \ll \lambda_w$, where λ_w is the wavelength of the perturbations, as well as the continuum approximation $\xi_i(t) = \xi(x, t)$, we have (Wei *et al.* 2023*a*)

$$\frac{\partial^2\xi}{\partial t^2} = B_1\left(\frac{\partial^2\xi}{\partial x^2} + \frac{a_0^2}{12}\frac{\partial^4\xi}{\partial x^4}\right) + B_2\frac{\partial\xi}{\partial x}\frac{\partial^2\xi}{\partial x^2}, \tag{2.1}$$

where $B_1 = k_1a_0^2/m_d$, $B_2 = 2k_2a_0^3/m_d$, $k_1 = (Q_d^2/4\pi\varepsilon_0a_0^3)e^{-\kappa}[2 + 2\kappa + \kappa^2]$, $k_2 = -(Q_d^2/8\pi\varepsilon_0a_0^4)e^{-\kappa}[6 + 6\kappa + 3\kappa^2 + \kappa^3]$, $\kappa = a_0/\lambda_D$.

3. Propagation characteristics of waves in an homogeneous dusty plasma

3.1. *Influence of the nonlinear parameter α on the propagation characteristics of the envelope wave*

In the following, we introduce the stretched coordinates $\eta = \varepsilon(x - Vt)$, $\tau = \varepsilon^2 t$ by using the traditional reductive perturbation method (Zhang *et al.* 2015; Gao *et al.*

https://doi.org/10.1017/S0022377826101354 Published online by Cambridge University Press

2017), where ε is a small parameter and V is the velocity of the wave. The quantity of ξ is expanded as $\xi = \sum_{n=1}^{\infty} \varepsilon^n \sum_{l=-\infty}^{+\infty} \xi^{(n,l)}(\eta, \tau) e^{il(kx-\omega t)}$.

Substituting these expansions into (2.1) and separation of terms according to the first three powers of ε yields dispersion relation of (see Appendix A) $\omega^2 = B_1 k^2[1 - (a_0^2/12)k^2]$, the group velocity of $V = B_1 k/\omega[1 - (a_0^2/6)k^2]$ and NLSE as follows: $i(\partial \xi^{(1,1)}/\partial \tau) + P(\partial^2 \xi^{(1,1)}/\partial \eta^2) + Q\xi^{(1,1)} \mid \xi^{(1,1)} \mid^2 = 0$, where $P = (2B_1 - 2V^2 - B_1 a_0^2 k^2)/4\omega$, $Q = 3B_2^2 k^6/(-12\omega^3 + 12\omega k^2 B_1 - 4\omega B_1 a_0^2 k^4)$. In the experimental coordinates, we have one envelope wave solution of NLSE as follows:

$$\xi_i = A\mathrm{sech}[w(x - Vt)]\mathrm{e}^{\mathrm{i}[k_b x - \omega_b t]}, \tag{3.1}$$

where $A = \varepsilon\sqrt{2(Pk^2 - \omega)/Q}$ is the envelope wave amplitude, $w = \varepsilon\sqrt{(Pk^2 - \omega)/P}$ the envelope wave width, V is the envelope wave group velocity and $k_b = k(\varepsilon + 1)$ the background wave frequency of the envelope wave, $\omega_b = (kV\varepsilon + \omega\varepsilon^2 + \omega)$. The envelope wave solution of (3.1) has been verified numerically and experimentally (Zhang *et al.* 2015; Gao *et al.* 2017; Jahan *et al.* 2019; Houwe *et al.* 2022).

To further explore the envelope wave solutions in this system, we assume that there is an arbitrary envelope wave as follows:

$$\xi_i = A\mathrm{sech}[\alpha w(x - Vt)]\mathrm{e}^{\mathrm{i}[k_b x - \omega_b t]}, \tag{3.2}$$

where α is an arbitrary constant. It is obvious that (3.2) is not a solution of the NLSE when $\alpha \neq 1$. However, in the present paper, we try to verify that the envelope wave expressed by (3.2) actually exist in the system.

To verify it, we perform a molecular dynamical simulations using the Large-scale Atomic/Molecular Massively Parallel Simulator (Sandia National Laboratories n.d.). We assume that each dust particle is a negative point charge and they are arranged as a chain. We place a chain of $N = 25\,000$ identical dust particles from $i = 0$ to $i = 24\,999$, and choose typical plasma and particle parameters according to the literature (Sun *et al.* 2018; Du *et al.* 2019; Huang *et al.* 2021): $a_0 = 0.8$ mm, $\lambda_D = 0.4$ mm, $Q_d = 2700e$, e represents the elementary charge, $m_d = 3.6 \times 10^{-15}$ kg and the diameter of each dust particle is $d = 1.55$ μm. The time step of the simulation is $\mathrm{d}t = 1.0 \times 10^{-4}$ s. For simplicity, we assume that the dust particle temperature is zero. We also assume that an envelope wave which satisfies (3.2) exists in the dusty lattice chain. Based on these assumptions, the initial displacements of all dust particles from their equilibrium positions and their corresponding velocities are determined from (3.2).

Figure 2 illustrates the temporal evolution of the velocity profile of an envelope wave in a one-dimensional dusty plasma chain under varying nonlinear parameter values (α = 0.5, 1.0, 5.0), which is given by (3.2). The parameter α inside the sech function is arbitrarily assigned. As α increases, the envelope becomes narrower and more localised. The consistency between analytical (solid lines) and numerical (dots) results confirms that such artificially constructed waveforms can propagate stably within the system.

The results presented in figure 2 demonstrate that the constructed envelop wave can propagate stably under various parameters α. It is an envelope solitary wave. However, there is a question whether it is a soliton. To verify it, we proceed to investigate head-on collisions between two envelop waves with different values of α.

There are two solutions of the dispersion relation $\omega^2 = B_1 k^2[1 - (a_0^2/12)k^2]$. We defined $\omega_1 = \sqrt{B_1(1 - (a_0^2/12)k^2)}k$, $\omega_2 = -\sqrt{B_1(1 - (a_0^2/12)k^2)}k$. When $\omega > 0$, the envelope wave propagates in the positive x-direction, whereas for $\omega < 0$, it propagates in the negative x-direction. Similarly, there are also two solutions of the group

https://doi.org/10.1017/S0022377826101354 Published online by Cambridge University Press

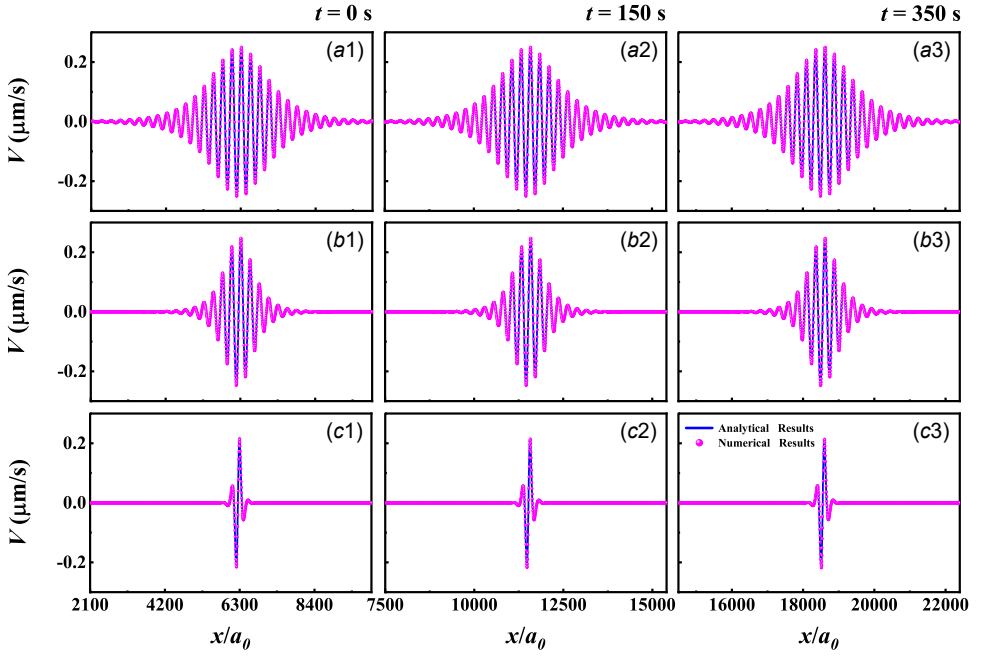


FIGURE 2. Comparison between MD simulation results and analytical results of envelope waves in a one-dimensional dusty particle chain under different parameters: (*a1–a3*) $\alpha = 0.5$, (*b1–b3*) $\alpha = 1.0$, (*c1–c3*) $\alpha = 5.0$) and at different times ($t = 150$ s and $t = 350$ s), which is given by (3.2). The analytical results are represented by blue solid lines, while the numerical ones are expressed by magenta dots.

velocity, $V_1 = B_1(k/\omega_1)[1 - (a_0^2/6)k^2]$, $V_2 = B_1(k/\omega_2)[1 - (a_0^2/6)k^2]$. Equation (3.2) can be written as

$$\xi_1 = \varepsilon\sqrt{\frac{2\left(P_{\omega_1}k^2 - \omega_1\right)}{Q_{\omega_1}}}\,\mathrm{sech}\left[\alpha_1\varepsilon\sqrt{\frac{\left(P_{\omega_1}k^2 - \omega_1\right)}{P_{\omega_1}}}(x - V_1 t)\right]\mathrm{e}^{\mathrm{i}[k(\varepsilon+1)x - \left(kV_1\varepsilon + \omega_1\varepsilon^2 + \omega_1\right)t]}, \tag{3.3}$$

$$\xi_2 = \varepsilon\sqrt{\frac{2\left(P_{\omega_2}k^2 - \omega_2\right)}{Q_{\omega_2}}}\,\mathrm{sech}\left[\alpha_2\varepsilon\sqrt{\frac{\left(P_{\omega_2}k^2 - \omega_2\right)}{P_{\omega_2}}}(x - V_2 t)\right]\mathrm{e}^{\mathrm{i}[k(\varepsilon+1)x - \left(kV_2\varepsilon + \omega_2\varepsilon^2 + \omega_2\right)t]}. \tag{3.4}$$

Equations (3.3) and (3.4) represent the envelope waves propagating in the positive and the negative x directions. Figure 3 illustrates the head-on collision of two envelope waves in a one-dimensional dusty plasma chain with differing parameters α. The initial displacements of all dust particles relative to their equilibrium positions, as well as the corresponding velocities, are determined by (3.3) and (3.4) and their time derivatives. In figure 3(*a1–a3*), the wave with $\alpha = 0.5$ collides with one of $\alpha = 1.0$, while in figure 3(*b1–b3*), $\alpha = 2.0$ collides with $\alpha = 1.0$. Numerical results (dots) closely align with analytical results (solid lines), verifying stable propagation and elastic-like interactions of artificially constructed waveforms. Despite differences in initial amplitudes and spatial widths due to the arbitrarily chosen

https://doi.org/10.1017/S0022377826101354 Published online by Cambridge University Press

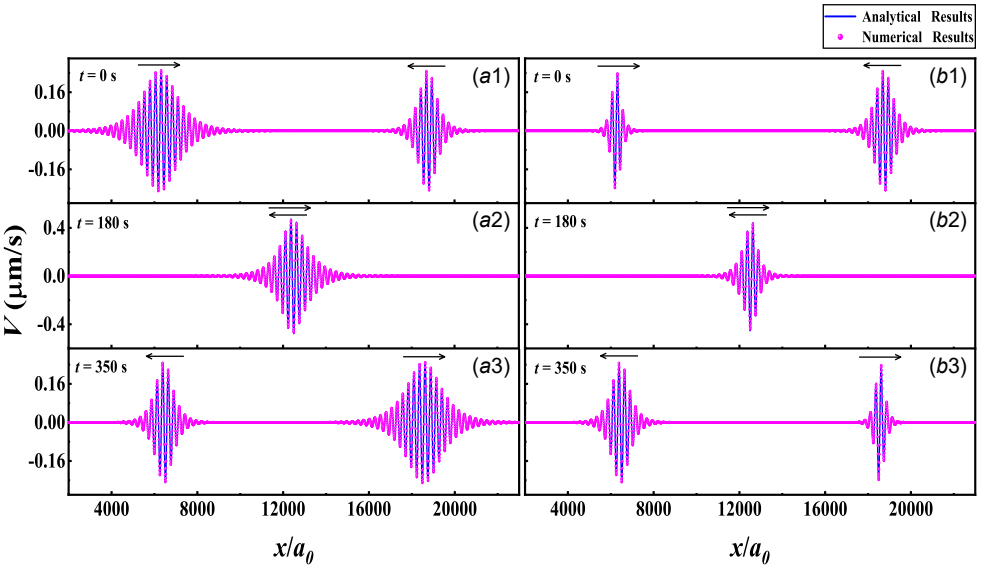


FIGURE 3. Head-on collision of two envelope waves in a one-dimensional dusty plasma chain with different parameters α at $t = 0$ s, 180 s and 350 s, which is given by (3.3) and (3.4). (*a1–a3*) Collision for $\alpha = 0.5$ and $\alpha = 1.0$, and (*b1–b3*) results for $\alpha = 2.0$ and $\alpha = 1.0$. The analytical results are represented by blue solid lines, while the numerical ones are expressed by magenta dots.

parameter α introduced in the sech function, the envelope waves maintain their structural integrity post-collision; this phenomenon conclusively demonstrates the robustness and waveform stability of these envelope waves under parameter α. The observed stability after the head-on collision between two waves indicates that both are solitons because the wave amplitudes, propagation velocities and wave widths all remain almost unchanged after the collision. These findings guide the design of stable soliton-based wave propagation in dusty plasmas and may enable tuneable signal transmission in microgravity experiments. In addition, these findings assist experimental control of wave collisions, facilitating adjustable waveform interactions in dusty plasma.

To further verify the soliton characteristics, apart from demonstrating the head-on collision between two envelope waves, figure 4 reveals that the product of the maximum amplitude A and the square of the envelope width L^2 remains nearly constant with time for different α. The results show that, for different α values, the product of the envelope amplitude A and the square of its width L^2 remains constant during the entire evolution process. This invariance is consistent with previous studies (Dharodi, Kumar & Sen 2023; Kumar *et al.* 2024).

To quantitatively evaluate the consistency between the numerical simulations and the analytical results from (3.2) for the constructed envelope waves, we next examine the relative error as a function of the parameter α. Figure 5 presents the variation of the relative error $|\Delta A|/A_{\max}$ between the numerical and analytical results for envelope waves as a function of the parameter α, evaluated at times $t = 150$ s and $t = 350$ s, where ΔA denotes the mean difference between the numerical and the analytical velocities of each dust particle derived from (3.2), and $A_{\max}$ refers to the maximum amplitude of the envelope wave at the initial moment. The error is shown

https://doi.org/10.1017/S0022377826101354 Published online by Cambridge University Press

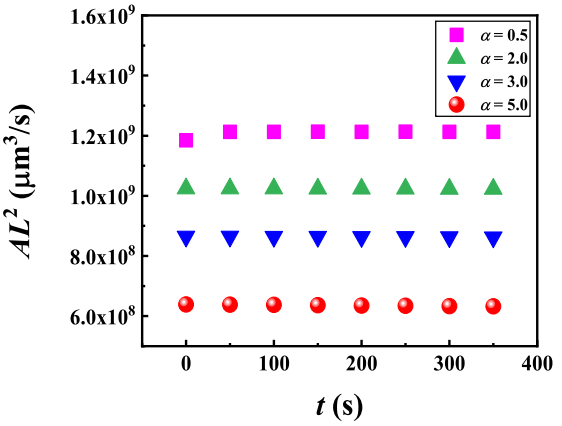


FIGURE 4. Dependence of the product of the maximum amplitude (A) and the square of the envelope width (L^2) as a function of time t for different α, as given by (3.2). The horizontal axis represents time t (s), and the vertical axis represents AL^2 ($\mu m^3\ s^{-1}$). Different colours correspond to different α values: $\alpha = 0.5$, 2.0, 3.0 and 5.0.

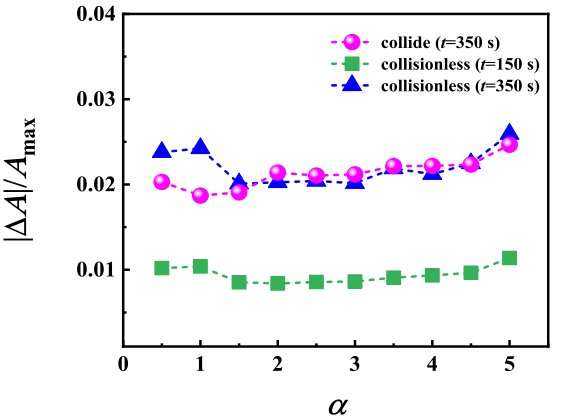


FIGURE 5. Relative error between the analytical and numerical results of the envelope wave at $t = 150$ s and $t = 350$ s varies with the parameter α. The relative error is defined as $|\Delta A|/A_{\max}$, where ΔA denotes the mean difference between the numerical and analytical velocities of each dust particle, and $A_{\max}$ refers to the maximum amplitude of the envelope wave at the initial moment. Magenta circles indicate the relative error at $t = 350$ s under collision conditions, green squares represent the error at $t = 150$ s without collision and blue triangles denote the error at $t = 350$ s without collision.

for both collisionless conditions (green squares and blue triangles) and collision conditions (magenta circles). The results reveal that the relative error increases with α, particularly in the collision scenarios. This increase is attributed to the enhanced nonlinear effects, which cause wavefront steepening and larger deviations from the theoretical results as α increases. The increasing relative error with α reflects the growing impact of nonlinearity, which steepens the soliton wavefront. As a result, the simulation accuracy decreases due to larger deviations from the analytical results, demonstrating the sensitivity of the system to nonlinear effects.

https://doi.org/10.1017/S0022377826101354 Published online by Cambridge University Press

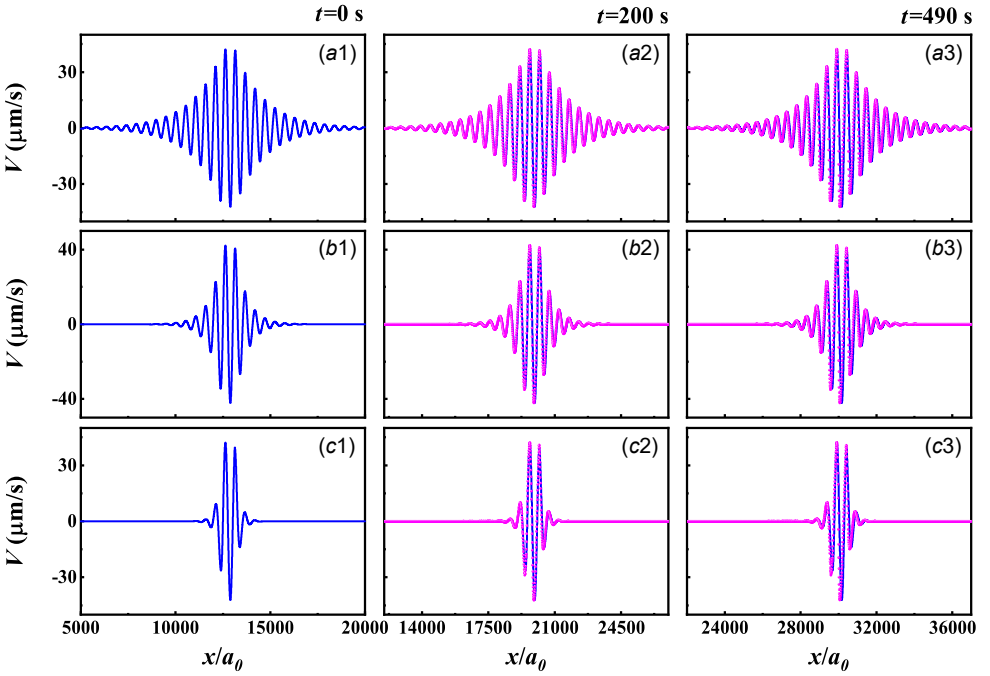


FIGURE 6. Comparison between the MD simulation results of waves in a one-dimensional dusty particle chain under different parameters: (*a1–a3*) $\alpha = 0.8$; (*b1–b3*) $\alpha = 2.0$; (*c1–c3*) $\alpha = 5.0$) and at different times ($t = 200$ s and $t = 490$ s), with the initial waveform at $t = 0$ s, which is given by (3.5). The waveform at the initial time is represented by blue solid lines, while the numerical ones are expressed by magenta dots.

3.2. *Propagation dynamics of a general wave*

Section 3.1 verifies the existence of the envelope wave represented by (3.2) in the system. We now proceed to examine whether a more general initial wave condition can stably evolve in the system, For this purpose, we assume that there is a wave which satisfy the following equation:

$$s_i = \begin{cases} A\cos\left[k(x-x_0)-\omega t\right]e^{\alpha(x-x_1)}, & 0 \leqslant x < x_1, \\ A\cos\left[k(x-x_0)-\omega t\right], & x_1 \leqslant x < x_2, \\ A\cos\left[k(x-x_0)-\omega t\right]e^{-\alpha(x-x_2)}, & x_2 \leqslant x. \end{cases} \tag{3.5}$$

Suppose that there are two waves. One is propagating in the positive x direction ($\omega > 0$), while the other is in the negative x direction ($\omega < 0$).

The initial position is set as $x_0 = 10$, $\Delta x = x_2 - x_1 = 0.5$, where ω satisfies the dispersion relation. The total number of dust particles is set to $N = 45\,000$. The initial displacements and velocities of all particles are calculated from (3.5) and its time derivative.

Figure 6 presents the temporal evolution of an initial perturbation wave in a one-dimensional dusty plasma chain under different parameters $\alpha = 0.8$, 2.0 and 5.0, which is given by (3.5). The waveforms at $t = 200$ s and $t = 490$ s are compared with that at $t = 0$ s, showing the evolution of the solitary waves. Notice that with increasing α, the wave experiences more pronounced steepening and deviation from its initial symmetric cosine shape. Particularly, higher α leads to faster amplitude

https://doi.org/10.1017/S0022377826101354 Published online by Cambridge University Press

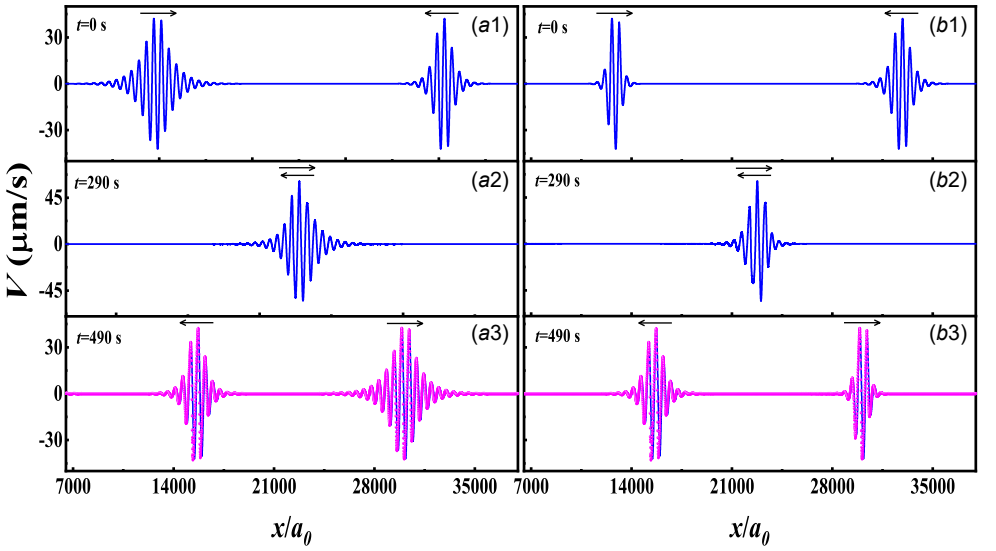


FIGURE 7. Head-on collision of two waves in a one-dimensional dusty plasma chain with different parameters α at $t = 0$ s, 290 s and 490 s, which is given by (3.5). (*a1–a3*) Collision for $\alpha = 1.4$ and $\alpha = 2.6$, and (*b1–b3*) results for $\alpha = 5.0$ and $\alpha = 2.6$. The waveform at the initial time is represented by blue solid lines, while the numerical ones are expressed by magenta dots.

modulation and more evident wavefront distortion, indicating that the nonlinearity critically controls the dispersive and modulational characteristics of the evolving wave structure.

Figure 7 displays the evolution of head-on collision between two waves in a one-dimensional dusty plasma chain under different nonlinear parameters α. Figure 7(*a1–a3*) depicts the case of $\alpha = 1.4$ and $\alpha = 2.6$, while figure 7(*b1–b3*) corresponds to $\alpha = 5.0$ and $\alpha = 2.6$. The velocity profiles are shown at $t = 0$, 180 and 490 s. After collision, the waves retain their general form, but exhibit minor amplitude fluctuations and phase shifts, especially for larger α. The results indicate that the interaction is weakly nonlinear and mostly elastic, with α influencing the post-collision waveform fidelity. The nonlinear parameter α modulates the balance between nonlinearity and dispersion, affecting wavefront steepness.

Figure 8 reveals that, for the wave described by (3.5), the product of the maximum amplitude A and the square of the wave width L^2 remains nearly constant with time for different α. This result demonstrates that the amplitude–width product is preserved throughout the entire evolution process, indicating robust soliton-like behaviour. This invariance is consistent with previous studies (Dharodi *et al.* 2023; Kumar *et al.* 2024).

Figure 9 illustrates the variation of the relative error of the wave described by (3.5) at $t = 200$ s and $t = 490$ s with respect to the nonlinear parameter α. The relative error is defined as $|\Delta A|/A_{\max}$. As α increases, the relative error also increases, particularly at later times. This suggests that higher values of α lead to greater nonlinearity, which causes deviations from the initial waveform. The increasing relative error with α reflects the enhanced nonlinearity, which causes wavefront steepening and amplifies deviations from the analytical solution slightly. These findings offer guidance for minimising errors in simulation, which improves wave propagation modelling, and in dusty plasma experiments.

https://doi.org/10.1017/S0022377826101354 Published online by Cambridge University Press

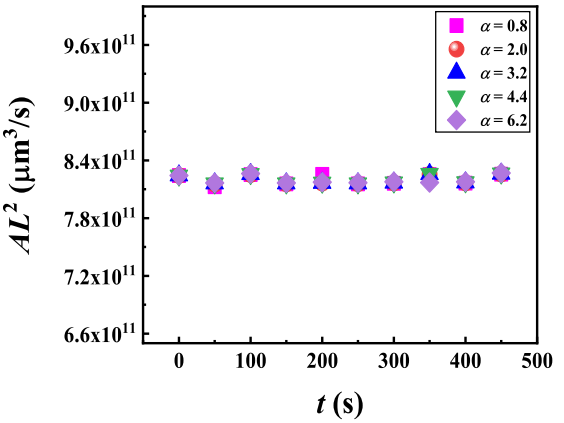


FIGURE 8. Dependence of the product of the maximum amplitude (A) and the square of the wave width (L^2) as a function of time t for different α, as given by (3.5). The horizontal axis represents time t (s) and the vertical axis represents AL^2 (μm^3 s^{-1}). Different colours correspond to different α values: $\alpha = 0.8$, 2.0, 3.2, 4.4 and 6.2.

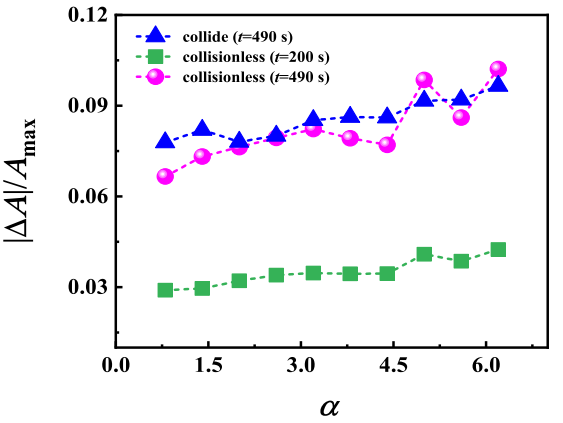


FIGURE 9. Variation of the relative error $|\Delta A|/A_{\max}$ between the numerical results of the wave obtained from (3.5) at $t = 200$ s and $t = 490$ s, and the initial waveform, with respect to the parameter α. The relative error is defined as $|\Delta A|/A_{\max}$, where ΔA represents the mean difference between the velocity of each dust particle and the initial time at different times, and $A_{\max}$ is the maximum amplitude of the wave at the initial time. Blue triangles represent the error at $t = 490$ s under collision conditions, magenta circles denote the relative error at $t = 490$ s without collision and green squares indicate the error at $t = 200$ s without collision.

4. Conclusion

This study investigates the existence, stability and interaction of non-standard envelope waves in one-dimensional dusty plasma chains. The results in the present paper are consistent with those in the previously reported ones, which studied the standard envelope solitons in dusty plasmas (Zhang *et al.* 2015; Rahman *et al.* 2018; Houwe *et al.* 2022). By combining analytical derivation using the NLSE and MD simulations, we verify the stable propagation of artificially modulated envelope solitons, even beyond the standard NLSE framework. Notably, envelope waves with varying

https://doi.org/10.1017/S0022377826101354 Published online by Cambridge University Press

widths maintain structural integrity and display elastic-like collisions, demonstrating soliton-like characteristics. These findings answer the paper's initial question regarding the existence and stability of arbitrary envelope waveforms in dusty plasma lattices, significantly extending prior work limited to analytical NLSE solutions.

The paper's primary contribution is demonstrating the stable existence and elastic-like collision of non-standard envelope waves in dusty plasma chains using MD simulations beyond conventional NLSE solitons. It introduces α as a tuneable parameter for envelope shaping and confirms robustness through precise error analysis. Crucially, it reveals that such envelope structures remain stable even when initially asymmetric, enriching the theoretical and practical understanding of nonlinear wave phenomena. This enables controlled waveform design in plasma-based applications, a novel insight for future experimental manipulation. The study advances nonlinear plasma physics by enabling customisable, stable waveform design for dusty plasmas.

Acknowledgements

The numerical calculations in this paper have been done on the supercomputing system in the Dongjiang Yuan Intelligent Computing Center.

Editor Edward Thomas, Jr. thanks the referees for their advice in evaluating this article.

Funding

This work was supported by the National Natural Science Foundation of China No. 12275223, the Gansu National Natural Science Foundation (24JRRP004) and the Innovation Fund for University Teachers in Gansu Province (2025A-212).

Declaration of interests

The authors report no conflicts of interest.

Data availability statement

The data that support the findings of this study are available within the article.

Appendix A. Reductive perturbation method for obtaining the first three powers of ε.

Here, we provide a detailed exposition of the key mathematical steps involved in the reductive perturbation method for obtaining the first three powers of ε. The quantity of ξ is expanded as (Gao *et al*. 2017; Lee 2010; Veeresha *et al*. 2010; Bala, Gill & Kaur 2012; Shalini & Misra 2015)

$$\xi = \sum_{n=1}^{\infty} \varepsilon^n \sum_{l=-\infty}^{+\infty} \xi^{(n,l)}(\eta, \tau) e^{il(kx-\omega t)}. \tag{A1}$$

By substituting these expansions into (2.1), we obtain the following equations corresponding to different orders of ε. At ε, we have

$$-l^2\omega^2 \sum_{l=-\infty}^{+\infty} \xi^{(1,l)} e^{il(kx-\omega t)} = B_1 \left[-l^2 k^2 \sum_{l=-\infty}^{+\infty} \xi^{(1,l)} e^{il(kx-\omega t)} + \frac{a_0^2}{12} l^4 k^4 \sum_{l=-\infty}^{+\infty} \xi^{(1,l)} e^{il(kx-\omega t)} \right]. \tag{A2}$$

https://doi.org/10.1017/S0022377826101354 Published online by Cambridge University Press

For $l = 1$, we can obtain the dispersion relation: $\omega^2 = B_1 k^2[1 - (a_0^2/12)k^2]$.

At ε^2,

$$
\begin{aligned}
&2il\omega V \sum_{l=-\infty}^{+\infty} \frac{\partial \xi^{(1,l)}}{\partial \eta} e^{il(kx-\omega t)} - l^2\omega^2 \sum_{l=-\infty}^{+\infty} \xi^{(2,l)} e^{il(kx-\omega t)} \\
&\quad = B_1 \left[2ilk \sum_{l=-\infty}^{+\infty} \frac{\partial \xi^{(1,l)}}{\partial \eta} e^{il(kx-\omega t)} - l^2k^2 \sum_{l=-\infty}^{+\infty} \xi^{(2,l)} e^{il(kx-\omega t)} \right] \\
&\qquad + \frac{a_0^2}{12} B_1 \left[l^4k^4 \xi^{(2,l)} e^{il(kx-\omega t)} - 4il^3k^3 \sum_{l=-\infty}^{+\infty} \frac{\partial \xi^{(1,l)}}{\partial \eta} e^{il(kx-\omega t)} \right] \\
&\qquad - B_2 ilk \sum_{l=-\infty}^{+\infty} \xi^{(1,l)} e^{il(kx-\omega t)} l^2k^2 \sum_{l=-\infty}^{+\infty} \xi^{(1,l)} e^{il(kx-\omega t)}. \qquad \text{(A3)}
\end{aligned}
$$

For $l = 1$, we can obtain the group velocity: $V = B_1(k/\omega)[1 - (a_0^2/6)k^2]$.

At ε^3,

$$
\begin{aligned}
&V^2 \sum_{l=-\infty}^{+\infty} \frac{\partial^2 \xi^{(1,l)}}{\partial \eta^2} e^{il(kx-\omega t)} + 2il\omega V \sum_{l=-\infty}^{+\infty} \frac{\partial \xi^{(2,l)}}{\partial \eta} e^{il(kx-\omega t)} - 2il\omega \sum_{l=-\infty}^{+\infty} \frac{\partial \xi^{(1,l)}}{\partial \tau} e^{il(kx-\omega t)} \\
&- l^2\omega^2 \sum_{l=-\infty}^{+\infty} \xi^{(3,l)} e^{il(kx-\omega t)} = B_1 \Bigg[\sum_{l=-\infty}^{+\infty} \frac{\partial^2 \xi^{(1,l)}}{\partial \eta^2} e^{il(kx-\omega t)} + 2ilk \sum_{l=-\infty}^{+\infty} \frac{\partial \xi^{(2,l)}}{\partial \eta} e^{il(kx-\omega t)} \\
&- l^2k^2 \sum_{l=-\infty}^{+\infty} \xi^{(3,l)} e^{il(kx-\omega t)} \Bigg] + \frac{a_0^2}{12} B_1 \Bigg[-6l^2k^2 \sum_{l=-\infty}^{+\infty} \frac{\partial^2 \xi^{(1,l)}}{\partial \eta^2} e^{il(kx-\omega t)} - 4il^3k^3 \sum_{l=-\infty}^{+\infty} \frac{\partial \xi^{(2,l)}}{\partial \eta} \\
&\times e^{il(kx-\omega t)} + l^4k^4 \sum_{l=-\infty}^{+\infty} \xi^{(3,l)} e^{il(kx-\omega t)} \Bigg] + B_2 \Bigg[ilk \sum_{l=-\infty}^{+\infty} \xi^{(1,l)} e^{il(kx-\omega t)} 2ilk \sum_{l=-\infty}^{+\infty} \frac{\partial \xi^{(1,l)}}{\partial \eta} \\
&\times e^{il(kx-\omega t)} - ilk \sum_{l=-\infty}^{+\infty} \xi^{(1,l)} e^{il(kx-\omega t)} l^2k^2 \sum_{l=-\infty}^{+\infty} \xi^{(2,l)} e^{il(kx-\omega t)} - \sum_{l=-\infty}^{+\infty} \frac{\partial \xi^{(1,l)}}{\partial \eta} e^{il(kx-\omega t)} \\
&\times l^2k^2 \sum_{l=-\infty}^{+\infty} \xi^{(1,l)} e^{il(kx-\omega t)} - ilk \sum_{l=-\infty}^{+\infty} \xi^{(2,l)} e^{il(kx-\omega t)} l^2k^2 \sum_{l=-\infty}^{+\infty} \xi^{(1,l)} e^{il(kx-\omega t)} \Bigg]. \qquad \text{(A4)}
\end{aligned}
$$

By simplification, we can obtain the NLSE:

$$
i \frac{\partial \xi^{(1,1)}}{\partial \tau} + P \frac{\partial^2 \xi^{(1,1)}}{\partial \eta^2} + Q \xi^{(1,1)} \mid \xi^{(1,1)} \mid^2 = 0, \qquad \text{(A5)}
$$

where $P = (2B_1 - 2V^2 - B_1 a_0^2 k^2/4\omega)$, $Q = (3B_2^2 k^6/ - 12\omega^3 + 12\omega k^2 B_1 - 4\omega B_1 a_0^2 k^4)$.

REFERENCES

AVINASH, K., ZHU, P., NOSENKO, V. & GOREE, J. 2003 Nonlinear compressional waves in a two-dimensional yukawa lattice. *Phys. Rev. E* **68**, 046402.

BALA, P., GILL, T.S. & KAUR, H. 2012 Ion-acoustic envelope excitations in multispecies plasma with non-thermally distributed electrons. *J. Plasma Phys.* **78**, 265–278.

https://doi.org/10.1017/S0022377826101354 Published online by Cambridge University Press

BANDYOPADHYAY, P., PRASAD, G., SEN, A. & KAW, P. 2008 Driven transverse shear waves in a strongly coupled dusty plasma. *Phys. Lett. A* **372**, 5467–5470.

BECKERS, J. *et al.* 2023 Physics and applications of dusty plasmas: the perspectives 2023. *Phys. Plasmas* **30**, 120601.

CHAUDHURI, M., IVLEV, A.V., KHRAPAK, S.A., THOMAS, H.M. & MORFILL, G.E. 2011 Complex plasmathe plasma state of soft matter. *Soft Matt.* **7**, 1287–1298.

CHU, J. & LIN, I. 1994 Direct observation of coulomb crystals and liquids in strongly coupled rf dusty plasmas. *Phys. Rev. Lett.* **72**, 4009.

DAVLETOV, A., KURBANOV, F. & MUKHAMETKARIMOV, Y.S. 2020 Influence of dust particles on ionization equilibrium in partially ionized plasmas. *Phys. Rev. E* **101**, 063203.

DHARODI, V., KUMAR, A. & SEN, A. 2023 Signatures of an energetic charged body streaming in a plasma. *Phys. Rev. E* **107**, 025207.

DING, X., LU, S., SUN, T., MURILLO, M. & FENG, Y. 2021 Head-on collision of compressional shocks in two-dimensional yukawa systems. *Phys. Rev. E* **103**, 013202.

DU, C.-R., *et al.* 2012 Experimental investigation on lane formation in complex plasmas under microgravity conditions. *New J. Phys.* **14**, 073058.

DU, C.-R., NOSENKO, V., THOMAS, H.M., LIN, Y.-F., MORFILL, G.E. & IVLEV, A.V. 2019 Slow dynamics in a quasi-two-dimensional binary complex plasma. *Phys. Rev. Lett.* **123**, 185002.

FAROKHI, B. & HAMEDITABAR, A. 2012 Comparison of dust lattice waves in three-dimensional cubic configurations. *Chin. Phys. Lett.* **29**, 025204.

FAROKHI, B., KOURAKIS, I. & SHUKLA, P. 2006 Dust lattice wave dispersion relations in two-dimensional hexagonal crystals including the effect of dust charge polarization. *Phys. Lett. A* **355**, 122–128.

GANDZHA, I. & SEDLETSKY, Y.V. 2017 Bright and dark solitons on the surface of finite-depth fluid below the modulation instability threshold. *Phys. Lett. A* **381**, 1784–1790.

GAO, D.-N., ZHANG, H., ZHANG, J., LI, Z.-Z. & DUAN, W.-S. 2017 Effect of a damping force on dust acoustic waves simulated by particle-in-cell method. *Phys. Plasmas* **24**, 043703.

GHOSH, S. 2008*a* Damped dust lattice shock wave in a strongly coupled complex (dusty) plasma. *JETP Lett.* **87**, 281–284.

GHOSH, S. 2008*b* Longitudinal dust lattice shock wave in a strongly coupled complex dusty plasma. *Contrib. Plasma Phys.* **48**, 569–576.

GHOSH, S. 2009 Shock wave in a two-dimensional dusty plasma crystal. *Phys. Plasmas* **16**, 103701.

GHOSH, S. & GUPTA, M. 2010 Solitary waves in two-dimensional dusty plasma crystal: effects of weak magnetic field. *Phys. Plasmas* **17**, 034505.

GONG, M., IVLEV, A.V., AKIMKIN, V. & CASELLI, P. 2021 Impact of magnetorotational instability on grain growth in protoplanetary disks. II. Increased grain collisional velocities. *Astrophys. J.* **917**, 82.

HAN, Y.-D., SHI, L.-X., YANG, Y.-Y. & DUAN, W.-S. 2025 Head on collision between two different kinds of nonlinear waves in a dusty plasma lattice chain. *Phys. Scr.* **100**, 085612.

HAVNES, O., ASLAKSEN, T., HARTQUIST, T., LI, F., MELANDSØ, F., MORFILL, G. & NITTER, T. 1995 Probing the properties of planetary ring dust by the observation of mach cones. *J. Geophys. Res. Space Phys.* **100**, 1731–1734.

HAYASHI, Y. & TACHIBANA, K. 1994 Observation of coulomb-crystal formation from carbon particles grown. *Jpn J. Appl. Phys.* **2**, L804–L806.

HOMANN, A., MELZER, A., PETERS, S., MADANI, R. & PIEL, A. 1998 Laser-excited dust lattice waves in plasma crystals. *Phys. Lett. A* **242**, 173–180.

HOMANN, A., MELZER, A., PETERS, S. & PIEL, A. 1997 Determination of the dust screening length by laser-excited lattice waves. *Phys. Rev. E* **56**, 7138.

HONG, X.-R., SUN, W., SCHWABE, M., DU, C.-R. & DUAN, W.-S. 2021 Reflection and transmission of an incident solitary wave at an interface of a binary complex plasma in a microgravity condition. *Phys. Rev. E* **104**, 025206.

HOUWE, A., ABBAGARI, S., INC, M., BETCHEWE, G., DOKA, S.Y. & CRÉPIN, K.T. 2022 Envelope solitons of the nonlinear discrete vertical dust grain oscillation in dusty plasma crystals. *Chaos Solitons Fractals* **155**, 111640.

https://doi.org/10.1017/S0022377826101354 Published online by Cambridge University Press

HUANG, H., IVLEV, A., NOSENKO, V., LIN, Y.-F. & DU, C.-R. 2019 Wave spectra of square-lattice domains in a quasi-two-dimensional binary complex plasma. *Phys. Plasmas* **26**, 013701.

HUANG, H., IVLEV, A.V., NOSENKO, V., YANG, W. & DU, C.-R. 2023 Dissipative solitary waves in a two-dimensional complex plasma: amorphous versus crystalline. *Phys. Rev. E* **107**, 045205.

HUANG, H., SCHWABE, M., THOMAS, H.M., LIPAEV, A.M. & DU, C.-R. 2021 Penetration of a supersonic particle at the interface in a binary complex plasma. *Phys. Rev. E* **103**, 013205.

IVLEV, A. & MORFILL, G. 2000 Anisotropic dust lattice modes. *Phys. Rev. E* **63**, 016409.

IVLEV, A., ZHDANOV, S. & MORFILL, G. 2003 Coupled dust-lattice solitons in monolayer plasma crystals. *Phys. Rev. E* **68**, 066402.

JAHAN, S., CHOWDHURY, N., MANNAN, A. & MAMUN, A. 2019 Modulated dust-acoustic wave packets in an opposite polarity dusty plasma system. *Commun. Theor. Phys.* **71**, 327.

JIANG, K. & DU, C.-R. 2022 Dynamics in binary complex (dusty) plasmas. *Rev. Mod. Plasma Phys.* **6**, 23.

KANANOVICH, A. & GOREE, J. 2020 Experimental determination of shock speed versus exciter speed in a two-dimensional dusty plasma. *Phys. Rev. E* **101**, 043211.

KARJANTO, N. 2022 Bright soliton solution of the nonlinear Schrödinger equation: Fourier spectrum and fundamental characteristics. *Mathematics* **10**, 4559.

KOMPANEETS, R., MORFILL, G.E. & IVLEV, A.V. 2016 Interparticle attraction in 2d complex plasmas. *Phys. Rev. Lett.* **116**, 125001.

KOUKOULOYANNIS, V., KEVREKIDIS, P., LAW, K., KOURAKIS, I. & FRANTZESKAKIS, D. 2010 Existence and stability of multisite breathers in honeycomb and hexagonal lattices. *J. Phys. A: Math. Theor.* **43**, 235101.

KOUKOULOYANNIS, V. & KOURAKIS, I. 2009 Discrete breathers in hexagonal dusty plasma lattices. *Phys. Rev. E Nonlinear Soft Matt. Phys.* **80**, 026402.

KOURAKIS, I. & SHUKLA, P.K. 2004 Nonlinear modulation of transverse dust lattice waves in complex plasma crystals. *Phys. Plasmas* **11**, 2322.

KOURAKIS, I. & SHUKLA, P.K. 2005 Discrete breather modes associated with vertical dust grain oscillations in dusty plasma crystals. *Phys. Plasmas* **12**, 014502.

KOURAKIS, I. & SHUKLA, P.K. 2006 Nonlinear excitations in strongly-coupled plasma lattices: envelope solitons, kinks and intrinsic localized modes. *Intl J. Bifurc. Chaos* **16**, 1711–1725.

KUMAR, K., BANDYOPADHYAY, P., SINGH, S. & SEN, A. 2024 Excitation of cylindrical and spherical precursor solitons in a flowing dusty plasma: experimental and simulation studies. *Phys. Plasmas* **31**, 023705.

LEE, N.C. 2010 Envelope equation of electrostatic nonlinear waves in relativistic two-fluid plasmas. *Phys. Plasmas* **17**, 082310.

LIAO, B., DONG, G., MA, Y. & MA, X. 2023 Numerical study on collisions of solitons of surface waves in finite water depth. *Fluids* **8**, 125.

LIPAEV, A.M., NAUMKIN, V.N., KHRAPAK, S.A., USACHEV, A.D., PETROV, O.F., THOMA, M.H., KRETSCHMER, M., DU, C.-R., KONONENKO, O.D. & ZOBNIN, A.V. 2025 Wave dispersion in a three-dimensional complex plasma solid under microgravity conditions. *Phys. Rev. E* **111**, 015209.

LIU, B., AVINASH, K. & GOREE, J. 2003 Transverse optical mode in a one-dimensional Yukawa chain. *Phys. Rev. Lett.* **91**, 255003.

LU, S., HUANG, D., LIANG, C. & FENG, Y. 2025 Internal friction of grain boundaries in two-dimensional Yukawa solids. *Phys. Rev. B* **111**, 174112.

MELANDSØ, F. 1996 Lattice waves in dust plasma crystals. *Phys. Plasmas* **3**, 3890–3901.

MELZER, A., TROTTENBERG, T. & PIEL, A. 1994 Experimental determination of the charge on dust particles forming Coulomb lattices. *Phys. Lett. A* **191**, 301–308.

MISAWA, T., OHNO, N., ASANO, K., SAWAI, M., TAKAMURA, S. & KAW, P. 2001 Experimental observation of vertically polarized transverse dust-lattice wave propagating in a one-dimensional strongly coupled dust chain. *Phys. Rev. Lett.* **86**, 1219.

MORFILL, G.E. & IVLEV, A.V. 2009 Complex plasmas: an interdisciplinary research field. *Rev. Mod. Phys.* **81**, 1353–1404.

NESPOLI, F. *et al.* 2022 Observation of a reduced-turbulence regime with boron powder injection in a stellarator. *Nat. Phys.* **18**, 350–356.

https://doi.org/10.1017/S0022377826101354 Published online by Cambridge University Press

NIU, Q., TIAN, M. & CHEN, H. 2020 Shock wave in one-dimensional dusty plasma crystal with charge gradient. *AIP Adv.* **10**, 095015.

NKENDJI KENKEU, E., TOGUEU MOTCHEYO, A., KANAA, T. & TCHAWOUA, C. 2022 Wave propagation with longitudinal dust grain oscillations in dusty plasma crystals. *Phys. Plasmas* **29**, 043702.

NUNOMURA, S., GOREE, J., HU, S., WANG, X., BHATTACHARJEE, A. & AVINASH, K. 2002 Phonon spectrum in a plasma crystal. *Phys. Rev. Lett.* **89**, 035001.

OMAR, F.M., MURAD, M.A.S., MAHMOOD, S.S., MALIK, S. & RADWAN, T. 2025 Optical solitons, bifurcation, and chaos in the nonlinear conformable Schrödinger equation with group velocity dispersion coefficients and second-order spatiotemporal terms. *Sci. Rep.* **15**, 20073.

OSBORNE, A.R. 2002 Nonlinear ocean wave and the inverse scattering transform. In *Scattering*, pp. 637–666.

OTANI, N.F., BHATTACHARJEE, A. & WANG, X. 1999 A unified model of acoustic and lattice waves in a one-dimensional strongly coupled dusty plasma. *Phys. Plasmas* **6**, 409.

POPEL, S. & DUBINSKY, A.Y. 2013 Dusty plasma processes in Earth's polar summer mesosphere. *J. Plasma Phys.* **79**, 383–385.

RAHMAN, M., CHOWDHURY, N., MANNAN, A., RAHMAN, M. & MAMUN, A. 2018 Modulational instability, rogue waves, and envelope solitons in opposite polarity dusty plasmas. *Chin. J. Phys.* **56**, 2061–2068.

Sandia National Laboratories n.d. LAMMPS molecular dynamics simulator. Available at: http://lammps.sandia.gov. (accessed 13 March 2026).

SANTOS, M., REEVES, B., MICHAEL, P., TAN, R., WISE, S.G. & BILEK, M.M. 2019 Substrate geometry modulates self-assembly and collection of plasma polymerized nanoparticles. *Commun. Phys.* **2**, 52.

SHALINI, SAINI, N, & MISRA, A. 2015 Modulation of ion-acoustic waves in a nonextensive plasma with two-temperature electrons. *Phys. Plasmas* **22**, 092124.

SHERIDAN, T., NOSENKO, V. & GOREE, J. 2008 Experimental study of nonlinear solitary waves in two-dimensional dusty plasma. *Phys. Plasmas* **15**, 073703.

SHI, L.-X., WEI, L., YANG, Y.-Y., YANG, L. & DUAN, W.-S. 2024 Theoretical investigation of wave transmission and reflection in a 1D dusty plasma chain with impurities. *Phys. Plasmas* **31**, 113701.

SHUKLA, P.K. & ELIASSON, B. 2009 Colloquium: fundamentals of dust-plasma interactions. *Rev. Mod. Phys.* **81**, 25–44.

SINGH, S., BANDYOPADHYAY, P., KUMAR, K. & SEN, A. 2022 Square lattice formation in a monodisperse complex plasma. *Phys. Rev. Lett.* **129**, 115003.

SLUNYAEV, A., CLAUSS, G.F., KLEIN, M. & ONORATO, M. 2013 Simulations and experiments of short intense envelope solitons of surface water waves. *Phys. Fluids* **25**, 067105.

STEPANYANTS, Y.A. 2019 Dynamics of internal envelope solitons in a rotating fluid of a variable depth. *Fluids* **4**, 56.

STERNOVSKY, Z., HOLZWORTH, R., HORÁNYI, M. & ROBERTSON, S. 2004 Potential distribution around sounding rockets in mesospheric layers with charged aerosol particles. *Geophys. Res. Lett.* **31**, L22101.

SUN, W. *et al.* 2018 Dissipative solitary wave at the interface of a binary complex plasma. *Europhys. Lett.* **122**, 55001.

THOMA, M.H., THOMAS, H.M., KNAPEK, C.A., MELZER, A. & KONOPKA, U. 2023 Complex plasma research under microgravity conditions. *NPJ Micrograv.* **9**, 13.

THOMAS, E., KONOPKA, U., MERLINO, R.L. & ROSENBERG, M. 2016 Initial measurements of two- and three-dimensional ordering, waves, and plasma filamentation in the magnetized dusty plasma experiment. *Phys. Plasmas* **23**, 055701.

THOMAS, H., MORFILL, G., DEMMEL, V., GOREE, J., FEUERBACHER, B. & MÖHLMANN, D. 1994 Plasma crystal: Coulomb crystallization in a dusty plasma. *Phys. Rev. Lett.* **73**, 652.

TIAN-JUN, F. 2009 Dissipation of nonlinear wave in inhomogeneous dust plasma crystal. *Commun. Theor. Phys.* **52**, 941.

TOGUEU MOTCHEYO, A., NKENDJI KENKEU, E., DJAKO, J. & TCHAWOUA, C. 2018 Backward-wave propagation with vertical dust grain oscillations in dusty plasma crystals. *Phys. Plasmas* **25**, 123701.

VEERESHA, B., TIWARI, S., SEN, A., KAW, P. & DAS, A. 2010 Nonlinear wave propagation in strongly coupled dusty plasmas. *Phys. Rev. E Nonlinear Soft Matt. Phys.* **81**, 036407.

https://doi.org/10.1017/S0022377826101354 Published online by Cambridge University Press

VLADIMIROV, S., SHEVCHENKO, P. & CRAMER, N. 1997 Vibrational modes in the dust-plasma crystal. *Phys. Rev. E* **56**, R74.

WANG, X.-Y., DUAN, W.-S., LIN, M.-M. & WAN, G.-X. 2006 Waves in three-dimensional simple cubic lattice. *Chaos Solitons Fractals* **30**, 909–919.

WAZWAZ, A.-M., ALYOUSEF, H.A., ISMAEEL, S.M. & EL-TANTAWY, S.A. 2023 Bright and dark optical modulated soliton solutions for the fourth-order $(2 + 1)$-dimensional Schrödinger equation with higher-order odd and even terms. *Optik* **277**, 170708.

WEI, L., PENG, Y., YANG, Y.-Y., DU, Y.-Z., YANG, L. & DUAN, W.-S. 2023*a* Existence of both compressional and rarefactive nonlinear solitary waves in a chain of dust particles. *Phys. Scr.* **98**, 075603.

WEI, L., PENG, Y., YANG, Y.-Y., YANG, L. & DUAN, W.-S. 2023*b* Shock waves in strongly coupled one-dimensional dusty plasmas under Yukawa interactions. *Phys. Plasmas* **30**, 093701.

WILLIAMS, J., ROYER, C., THAKUR, S.C., THOMAS JR., E. & WILLIAMS, S. 2025 Measurement of the properties of the dust acoustic wave in a magnetic field. *J. Plasma Phys.* **91**, E15.

ZHANG, H., QI, X., DUAN, W.-S. & YANG, L. 2015 Envelope solitary waves exist and collide head-on without phase shift in a dusty plasma. *Sci. Rep.* **5**, 14239.

https://doi.org/10.1017/S0022377826101354 Published online by Cambridge University Press